Optimizing MRI for Radiation Oncology: Initial Investigations

James Balter[1]; Yue Cao[1]; Hesheng Wang[1]; Ke Huang[1]; Shu-Hui Hsu[1]; Martin Requardt[2]; Steven M. Shea[3]

[1] Department of Radiation Oncology, University of Michigan, Ann Arbor, MI, USA
[2] Siemens Healthcare, Erlangen, Germany
[3] Siemens Corporation, Corporate Technology, Baltimore, USA

Introduction

The superior soft tissue contrast, as well as potential for probing molecular composition and physiological behavior of tumors and normal tissues and their changes in response to therapy, makes MRI a tempting alternative to CT as a primary means of supporting the various processes involved in radiation therapy treatment planning and delivery. Obvious examples of the benefit of MRI over CT include target delineation of intracranial lesions, nasopharyngeal lesions, normal critical organs such as the spinal cord, tumors in the liver, and the boundaries of the prostate gland and likely cancerous regions within the prostate gland. For brachytherapy planning for cervical cancer, a recent GEC-ESTRO report directly recommends a change from traditional point-based prescriptions based primarily on applicator geometry, to volumetric treatment plans and prescriptions aided by soft tissue visualization, specifically improved by the use of MRI. MRI-based maps of diffusion and perfusion have demonstrated potential for predicting therapeutic outcome for tumors as well as normal tissues, and current clinical trials seek to validate their roles and performance as a means to individualize therapy to improve outcomes (minimize toxicity and improve local tumor control). In addition to these advantages, MRI has been initially investigated as a means to better map the movement and deformation of organs over time and due to physiological processes such as breathing.

The historically accepted challenges in using MRI for primary patient modeling in radiation oncology have included distortion, lack of electron density information, and lack of integrated optimized systems to scan patients immobilized in treatment configuration.

MRI 'simulator' system

Over the past several years, we have investigated the feasibility of MRI systems to function in the same roles that CT scanners have for the past 10–15 years, that is as primary tools for patient modeling for radiation therapy. These efforts have accelerated in the past years with the installation of a dedicated MRI 'simulator' at the University of Michigan, based on a 3T wide-bore scanner (MAGNETOM Skyra, Siemens Healthcare, Erlangen, Germany), outfitted with a laser marking system (LAP, Lueneburg, Germany) and separate detachable couch tops supporting brachytherapy and external beam radiation therapy applications.

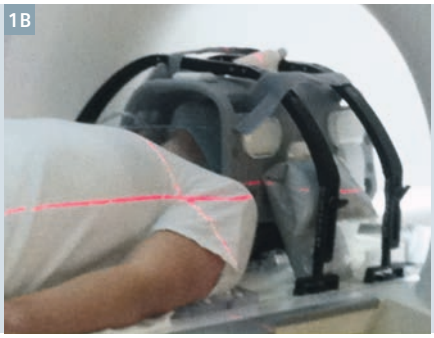

1

MRI simulation system shows a volunteer in position for initial setup wearing a customized face mask **(1A)**. Close-up view of anterior coil setup and crosshairs from laser marking system **(1B)**.

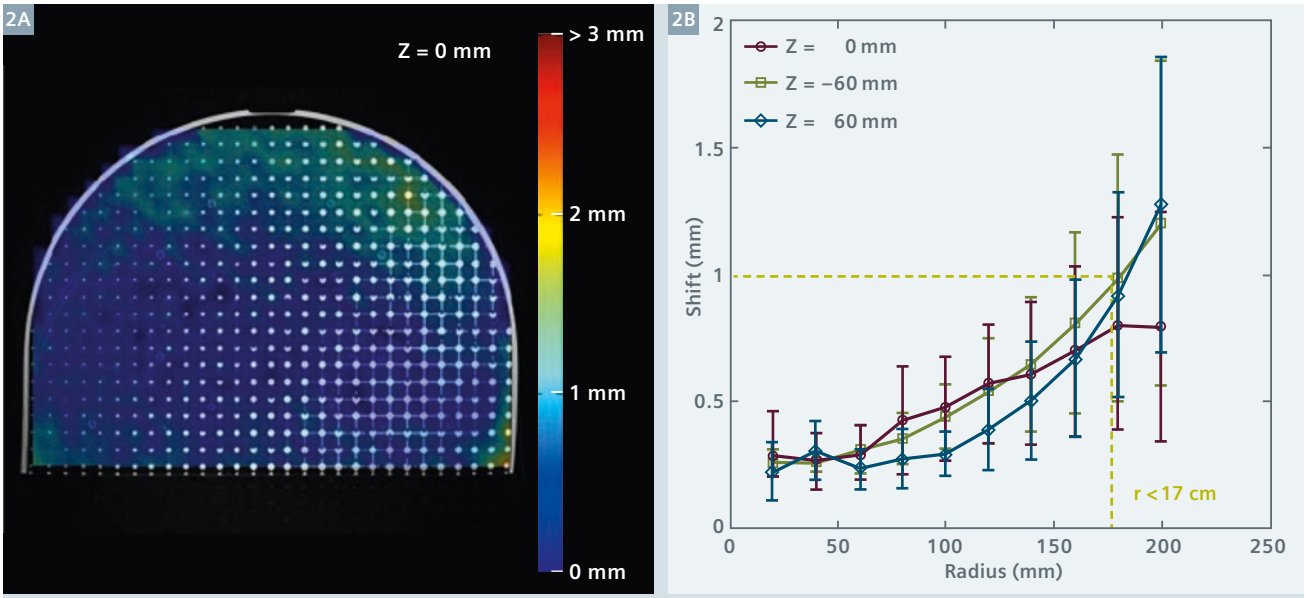

2 Colorwash of measured distortion through an axial plane of the distortion phantom **(2A)**. Magnitude of distortion-induced shifts in circles of increasing radius from the bore center in axial planes at the center and +/– 6 cm along the bore **(2B)**.

The process of integrating MRI into the standard workflow of radiation oncology requires attention be paid to a number of specific areas of system design and performance. In our instance, we chose a system that could potentially support both external beam therapy as well as brachytherapy. The brachytherapy requirement played a specific role in some of our design choices. As the high-dose-rate (HDR) brachytherapy system was housed in a room across the hall from the MRI suite, a room design was created that permitted the direct transfer of patients from MRI scanning to treatment. Typically brachytherapy treatment has involved transferring patients to and from imaging systems, a process that could potentially influence the treatment geometry and changes the dose delivered away from that planned. Treating a patient directly without moving them has significant advantages for geometric integrity as well as patient comfort. To facilitate such treatments, a detachable couch was chosen as part of the magnet specifications, and two such couches were specifically purchased to support simultaneous treatment of patients on the couch used for MRI scanning and scanning of other patients for subsequent external beam treatments.

To support external beam radiotherapy, patients need to be scanned in positions and configurations that can be reproduced at treatment. In addition to necessitating a wide bore MRI scanner, an indexed flat table top insert was purchased from a company that specializes in radiation therapy immobilization systems (Civco, Kalona, IA, USA). A number of immobilization accessories were customized for use in the MRI environment, most notably a head and neck mask attachment system. To support high quality scanning of patients in treatment position without interfering with their configuration for treatment, a series of attachments to hold surface coils (primarily 18-channel body coils) relatively close to the patient without touching are used.

Initial commissioning and tests

To commission the system, a number of tests were performed in addition to the standard processes for MRI acceptance and quality assurance. The laser system was calibrated to the scanner coordinates through imaging of a phantom with externally visible laser alignment markings and internal MRI-identifiable coordinates indicating the nominal laser intersection, and end-to-end tests were performed on phantoms and volunteers to establish the accuracy of isocenter marking using MRI scans as a source of input.

To characterize system-level distortion, a custom phantom was developed to fill the bore of the magnet (with perimeter space reserved for testing the 18-channel body coil if desired). The resulting phantom was a roughly cylindrical section with a sampling volume measuring 46.5 cm at the base, with a height of 35 cm, and a thickness of 16.8 cm. This sampling volume was embedded with a three-dimensional array of interconnected spheres, separated by 7 mm center-to-center distances. The resulting system provided a uniform grid of 4689 points to sample the local distortion. The phantom was initially scanned using a 3D, T1-weighted, spoiled gradient echo imaging sequence (VIBE, TR 4.39 ms and TE 2.03 ms, bandwidth 445 Hz/pixel) to acquire a volume with field-of-view of 500 × 500 × 170 mm with a spatial resolution of 0.98 × 0.98 × 1 mm. Standard 3D shimming was used for scanning, and 3D distortion correction was applied to the images prior

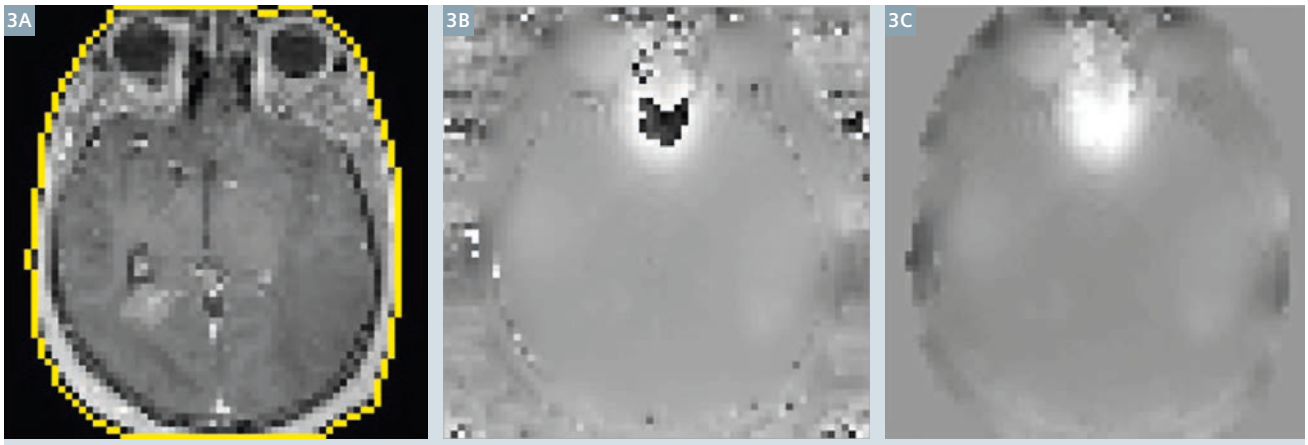

3 T1-weighted image with external contour delineated as a mask **(3A)**. The B_0 inhomogeneity map acquired from this subject **(3B)** was unwrapped within the boundaries of the mask, yielding the resulting distortion map **(3C)**.
Reprinted with permission from Wang H, Balter J, Cao Y. Patient-induced susceptibility effect on geometric distortion of clinical brain MRI for radiation treatment planning on a 3T scanner. Phys Med Biol 58(3):465-77, 2013.

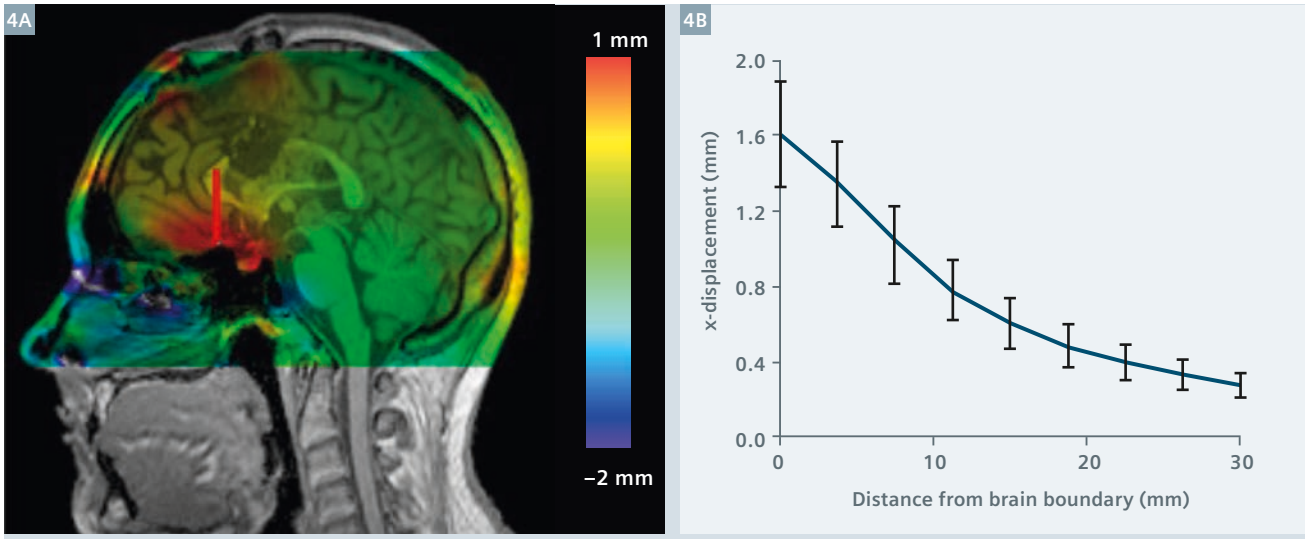

4 Colorwash of distortion-induced displacements through a sagittal plane of a subject **(4A)**. Analysis of displacements along a line moving away from the sinus (red line in fig. 4A) shows the falloff of distortion due to susceptibility differences as a function of distance from the interface **(4B)**.
Reprinted with permission from Wang H, Balter J, Cao Y. Patient-induced susceptibility effect on geometric distortion of clinical brain MRI for radiation treatment planning on a 3T scanner. Phys Med Biol 58(3):465-77, 2013.

to analysis. For this initial test, the body coil integrated into the magnet was used. Automated analysis of the images localized the sphere centers, yielding a deformation vector field that described the influence of system-level distortion on the measured sphere locations. This initial test demonstrated the accuracy of coordinate mapping via this scanning protocol, with average 3D distortions of less than 1 mm at radii of up to 17 cm in planes through the bore center as well as +/– 6 cm along the bore length. Of note, scanning was performed using the *syngo* MR D11 software version. Future tests will be performed on the *syngo* MR D13 release.

To begin to assess the impact of subject-induced susceptibility on distortions, B_0 inhomogeneity maps were acquired during routine patient scanning and analyzed (for 19 patients) under an IRB-approved protocol. These maps were acquired using a 2D, double-echo, spoiled gradient echo sequence (GRE field mapping TE_1 4.92 ms, TE_2 7.38 ms, TR 400 ms, flip angle 60 degrees, voxel size 3.5 × 3.5 × 3.75 mm), masked by the boundaries of the head acquired from T1-weighted images, and unwrapped using an algorithm from the Oxford Center for Functional Magnetic Resonance Imaging of the Brain [1]. The resulting maps showed homogeneity

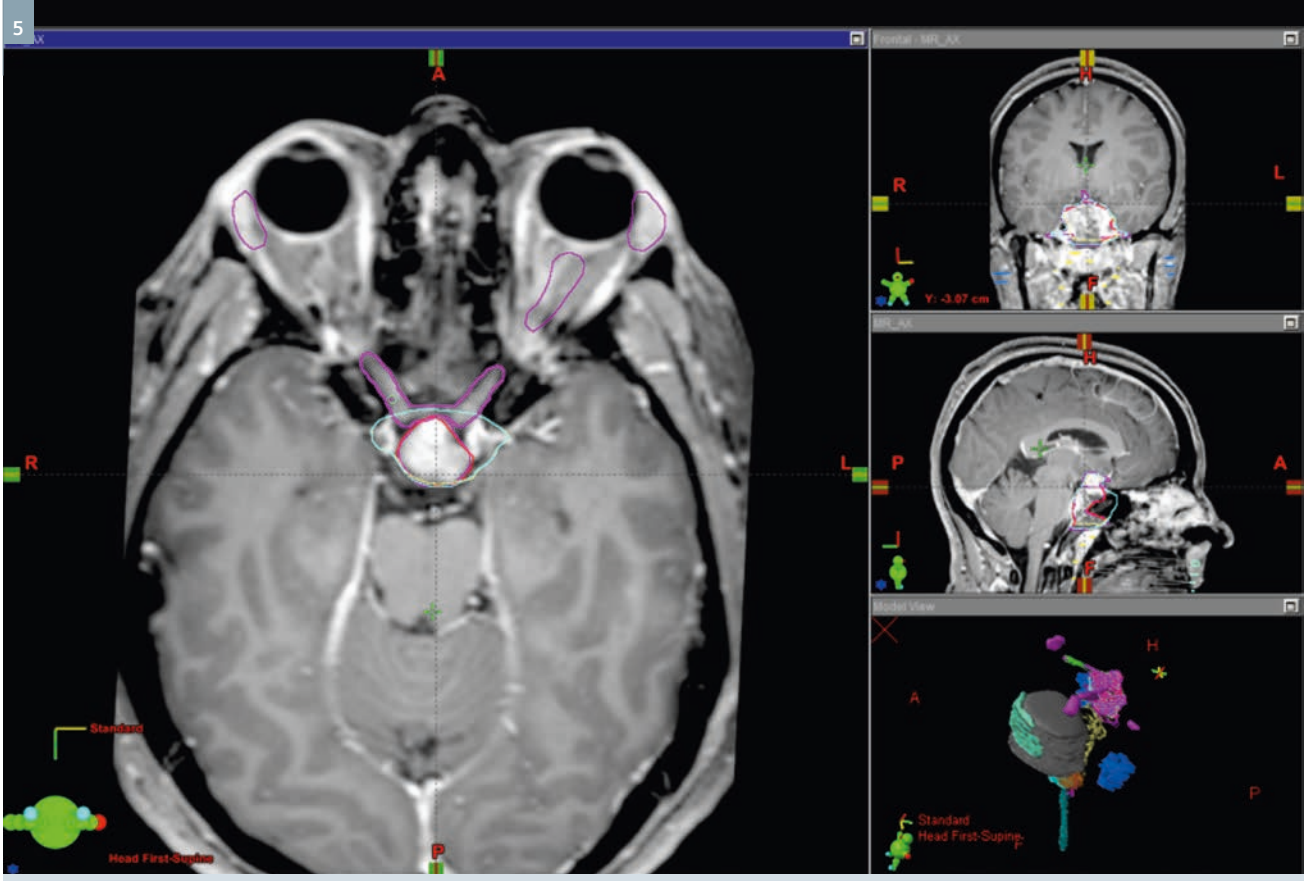

5 Post-contrast T1-weighted images of a patient scanned in an immobilization mask using an anterior 18-channel body surface coil and a posterior 4-channel small soft coil and displayed in a radiation therapy treatment planning system (Eclipse, Varian, Palo Alto, CA, USA). Various delineated structures shown are used to guide optimization of intensity-modulated radiation therapy.

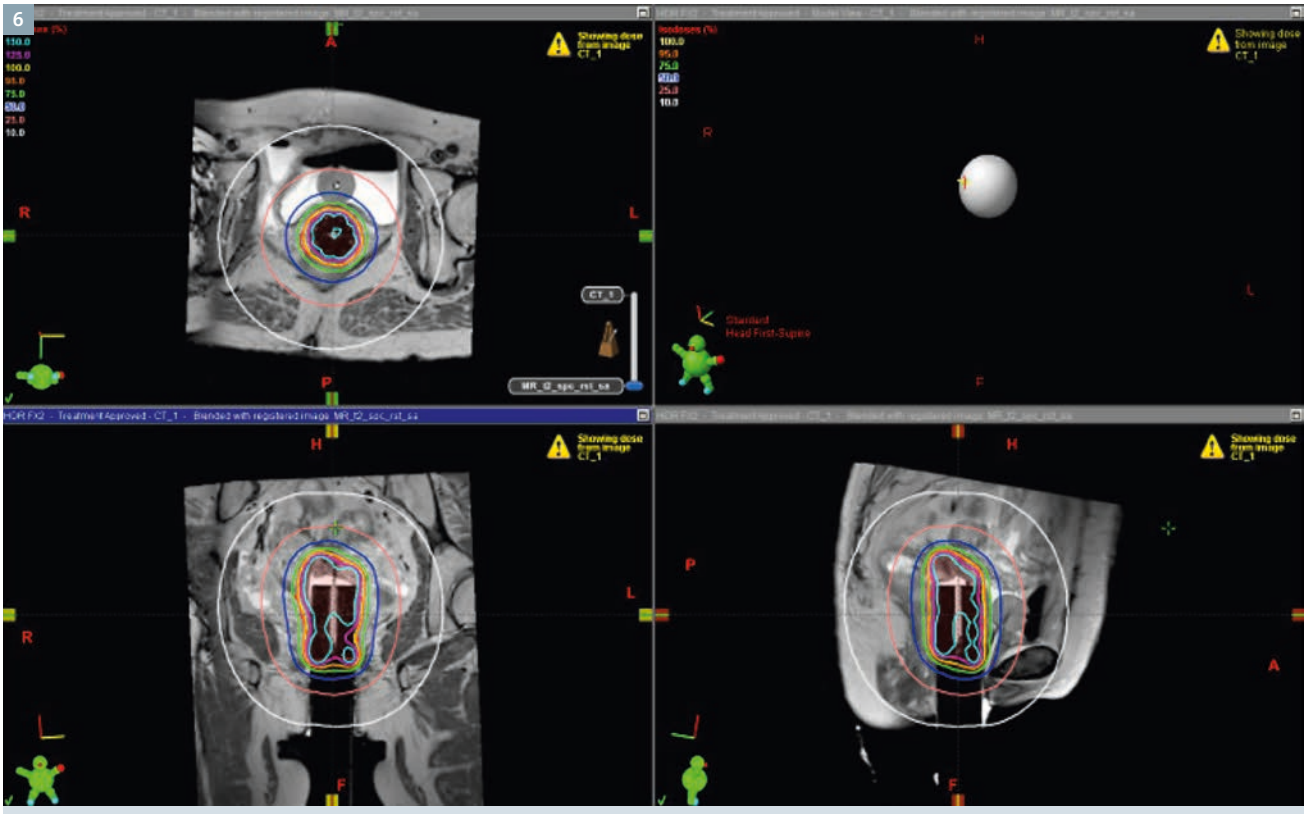

6 Display from a brachytherapy treatment planning system (Brachyvision, Varian, Palo Also, CA, USA) showing orthogonal planes through cylindrical applicator implanted in a patient. Source locations (red dashes through the center of the applicator) are shown, as well as radiation isodose lines.

of 0.035 ppm or less over 88.5% of a 22 cm diameter sphere, and 0.1 ppm or less for 100% of this volume.

These inhomogeneity maps were applied to calculate distortions from a typical clinical brain imaging sequence (3D T1-weighted MPRAGE sequence with TE 2.5 ms, Siemens TR 1900 ms, TI 900 ms, flip angle 9 degrees, voxel size 1.35 × 1.35 × 0.9 mm, frequency-encoding sampling rate of 180 Hz/pixel). On these images, 86.9% of the volume of the head was displaced less than 0.5 mm, 97.4% was displaced less than 1 mm, and 99.9% of voxels exhibited less than 2 mm displacement. The largest distortions occurred at interfaces with significant susceptibility differences, most notably those between the brain and either metal implants or (more significantly) adjacent air cavities. In the location with the largest displacement (interface with the sinus), the average displacement of 1.6 mm at the interface falls to below 1 mm approximately 7 mm away.

Examples of clinical use

We have implemented a number of scanning protocols in our first year of operation. Routine scans are performed for patients with intracranial lesions of all forms, as well as for those with nasopharyngeal tumors, hepatocellular carcinoma, and certain spinal and pelvic lesions. Routine use of the system for MRI-based brachytherapy of patients with cervical cancer using a ring and tandem system is currently pending modification of part of the applicator for safety and image quality reasons, although patients undergoing other implants (e.g. cylinders) have had MRI scans to support treatment planning.

Summary

We have implemented the initial phase of MRI-based radiation oncology simulation in our department, and have scanned over 300 patients since operations began just over one year ago. The system demonstrates sufficient geometric accuracy for supporting radiation oncology decisions for external beam radiation therapy, as well as brachytherapy. Work is ongoing in optimizing MRI scanning techniques for radiation oncology in various parts of the body and for various diseases. In addition to current and future work in optimizing MRI for use in routine radiation therapy, a variety of research protocols are underway using this system. A major current focus is on using MRI without CT for external beam radiation therapy. Results of these efforts will be presented in future articles.

References

1 Jenkinson M. Fast, automated, N-dimensional phase-unwrapping algorithm. Magn Reson Med. 2003 Jan;49(1):193-7.

2 Dimopoulos JC, Petrow P, Tanderup K, Petric P, Berger D, Kirisits C, Pedersen EM, van Limbergen E, Haie-Meder C, Pötter R. Recommendations from Gynaecological (GYN) GEC-ESTRO Working Group (IV): Basic principles and parameters for MR imaging within the frame of image based adaptive cervix cancer brachytherapy. Radiother Oncol 103(1):113-22, 2012.

3 Wang H, Balter J, Cao Y. Patient-induced susceptibility effect on geometric distortion of clinical brain MRI for radiation treatment planning on a 3T scanner. Phys Med Biol 58(3):465-77, 2013.

Contact

James M. Balter, Ph.D., FAAPM
Professor and co-director,
Physics division
Department of Radiation Oncology
University of Michigan
Ann Arbor, MI
USA
Phone: +1(734)936-9486
jbalter@umich.edu